Ultrahigh fluid diffusivity in graphene-lined nanochannels

Shishir Kumar, Rudra Pratap, and Srinivasan Raghavan

Citation: Appl. Phys. Lett. **108**, 091606 (2016); doi: 10.1063/1.4943085
View online: http://dx.doi.org/10.1063/1.4943085
View Table of Contents: http://aip.scitation.org/toc/apl/108/9
Published by the American Institute of Physics

Ultrahigh fluid diffusivity in graphene-lined nanochannels

Shishir Kumar,[a] Rudra Pratap, and Srinivasan Raghavan
Centre for Nanoscience and Engineering, Indian Institute of Science, Bangalore 560012, India

(Received 17 November 2015; accepted 19 February 2016; published online 4 March 2016)

Control and understanding of the flow of fluids at nanoscales is of great significance to biology, separation science, energy technology, and medical diagnostics. Nanocarbons have emerged as one of the most promising materials for this quest, both as nanochannels and nanoporous membranes. However, the fluid flow in these graphitic nanostructures is not well understood, and there is a lack of straightforward route for process integration of the nanochannels. The graphene-lined nanochannels (GNCs), reported here, are aimed at solving these problems, while displaying a useful anomaly for fluidic flow. Specifically, GNCs show a large increase in the rate of removal of sacrificial materials enclosed in them. The increase is caused by 100–1000 times enhancement in the diffusivity of etchant media in the GNCs as compared to channels without graphene lining. The enhancement increases monotonically with a decrease in the height of the GNCs, which is not seen for the non-lined channels. These properties, coupled with easy and scalable fabrication, make GNCs highly suited for innovative and efficient nanofluidic devices and also for experimental investigations. We also provide a phenomenological model which assumes enhanced diffusivity of medium only near graphene surface to explain the observed dependence of diffusivity on the dimensions of the nanochannels. This rationalization of the phenomenon using only the surface effects is a significant step towards understanding anomalous fluidics of nanocarbons. © *2016 AIP Publishing LLC*.
[http://dx.doi.org/10.1063/1.4943085]

The fluid flow at nanoscale results from interplay of a variety of physical effects.[1–3] Better understanding of nanofluidics, thus, requires nanostructured devices which can be well controlled and offer considerable flexibility of experimental conditions. At the same time, such devices can help in designing efficient and perhaps novel solutions to critical problems in domains like separation, biochemical analysis, and energy harvesting. Carbon can be nanostructured and modified in myriad ways, which make it highly suited for implementing such devices. Carbon forms also display extraordinary fluidic properties,[4–10] which can be tuned,[11] but many applications are marred by the lack of straightforward process for their large scale integration and mechanistic understanding of the said properties.

In this light, graphene offers considerable advantages for nanofluidic implements. It can be produced on a large scale and is compatible with the standard thin film processing. Also, as a graphitic nanocarbon, it inherits chemical versatility of carbon and possibly the anomalous fluid flow properties displayed by nanocarbons. Despite these promises, graphene has not been explored for making nanochannels.

Graphene-lined nanochannels (GNCs) fill this void and importantly, display a useful fluid flow anomaly of graphene. By observing the etching of straight lines of sacrificial materials (SMs) contained in GNCs, we show that the diffusivity of etchant media is enhanced by 100–1000 times over those in channels without graphene. GNCs containing different SMs—a metal, a polymer, and a ceramic—display similar enhancements, indicating that the phenomenon is related to fluidic effects rather than the chemical identities involved in the process. Curiously, GNCs show increase in diffusivities when the height of channel is reduced, which is not seen for the reference samples.

This dependence can be explained by a phenomenological model, which assumes higher diffusivity of etchant media in a layer near the graphene surface. The model also constrains the thickness of the layer to be independent of the channel height, emphasizing the role of interactions between the fluid molecules and graphene surface. These results are in agreement with the recent predictions of ultrafast diffusion of water nanodroplets on graphene.[12] GNCs provide a well controlled platform for investigating the theory further.

Additionally, the scope of these experiments extends to studying anomalous fluidic behavior seen with other graphitic nanocarbons. Similar to enhancement of fluid flow in carbon nanotubes (CNTs), recent reports have suggested very high flow rates of fluids between stacked flakes of graphene or graphene-oxide.[13,14] As the dynamic friction can be related to diffusivity by a Stokes-Einstein type of relation, a link is implied between the anomalous flow in these nanocarbons to anomalous diffusivity in GNCs. Understanding the latter will improve the understanding of the former.

Our experiments also resolve a curiosity noted by Bolotin *et al.*[15] These authors found that the etching action of HF on SiO_2 was faster under graphene, compared to the areas where SiO_2 was covered with other materials. This occurrence is similar to what we observe here.

The enhanced diffusivity of fluids in GNCs can be useful in many ways. It will allow easier movement of large molecules, e.g., polymers in confined nanochannels, which can make bioanalysis in nanochannels more efficient.[16] Such channels can also lead to novel devices,[17,18] and efficient chromatographic and fluid separation.[2]

[a]Author to whom correspondence should be addressed. Electronic mail: shishirk@gmail.com

The test samples contained straight lines of a SM encapsulated in graphene and protected by a transparent, impermeable, and robust layer on both sides (Figures 1(a) and 1(b) with Cr as SM). The reference samples were exactly the same, but without graphene. Cr was evaporated and lithographically patterned as straight lines on graphene lying on the SiO_2 (300 nm) coated Si wafer. Another layer of graphene was transferred, followed by evaporation of 100 nm SiO_2. To guard against pinholes in the final SiO_2 layer, it was capped by annealed photoresist film (APF).[19] In the reference samples, no graphene was used and so, Cr lines were in direct contact with SiO_2 layers on both sides. We also tested samples having SiO_2 and LOR (a polymer, Lift-Off Resist) as sacrificial lines. These samples have different encapsulation materials compatible to the etchants used.[19] The monolayer chemical vapor deposited graphene was used in the experiments. It was grown on copper and transferred using polymer support by the standard techniques.[19] The width w and height d of SM lines were in tens of μm and $\sim<100$ nm, respectively. The height of the lines was determined by atomic force microscopy, which also confirmed the surface smoothness after deposition of the graphene layer (Figure 1(d)).

The as made samples were broken into pieces to expose the SM core in the cross-section. When these pieces were dipped in an etchant for the SM, a tunnel was formed in the encapsulation layer, which elongated with time (Figure 1(c)). The etched length of SM, $x(t)$, was monitored as a function of time by periodically taking the sample out of the etchant and optically imaging it.[19] The mechanical strength of SiO_2 and APF makes the channels robust against collapse, and we observed a repeatable increase in $x(t)$ with time. The time taken by the etchant medium to fill an already formed channel is small. It is driven by capillary filling and aided by the removal of entrapped gas by dissolution in the advancing liquid.[20] Studies on Si nanochannels[21,22] indicate that the time for capillary filling of 1 mm long, one-side closed nanochannels should be smaller than 10 s, which is only a small fraction of time intervals used below. We also confirmed that the frequent removal of samples from the etchant did not affect the results significantly.[19] There was no infiltration of etchant between the other interfaces for any samples, as the etch action advanced only along the lines and not radially in all directions.

Figures 1(e) and 1(f) show the optical micrographs of Cr lines encapsulated in evaporated SiO_2 and etched with cerium ammonium nitrate (CAN, Technic No. 1 etchant). In the test sample (Figure 1(e)), the nanochannels formed at a rate that was $\sim$100 times faster than that in the reference sample (Figure 1(f)). The dependence of $x(t)$ on time is plotted in Figure 1(g) for the two samples, contrasting the large difference. To test whether the graphene present in test sample is responsible for the faster removal of SM, we observed a sample with 20 nm thick Cr lines, broken into two pieces. One piece was observed as above. The other piece was subjected to O_2 plasma treatment for 2 min, after etching in Cr etchant for $\sim$5 min. The plasma treatment removes or degrades the exposed graphene lining from the already formed nanochannels. Figure 1(h) shows that both pieces were experiencing the same removal rates, till plasma treatment was applied. After that point, the removal rate of the treated piece slowed down to that of the reference sample level. Similar behaviour was seen with the test samples having 150 nm thick Cr lines (Figure 1(h)), indicating that plasma has access to nanochannel interior.

We repeated the experiments LOR and SiO_2 as SMs. SiO_2 was etched with dilute HF (buffered oxide etch). LOR can either be etched with a basic developer (we used tetramethyl ammonium hydroxide, TMAH) or can be physically dissolved in an organic solvent (ethyl lactate, EL) after it has been exposed to deep UV radiation. Again, we see that the graphene lined channels display faster removal of SM (Figure 2). It is also notable that the level of enhancement is similar in all cases, despite differences in the liquids involved. The enhancement of the removal rate of LOR in EL is particularly

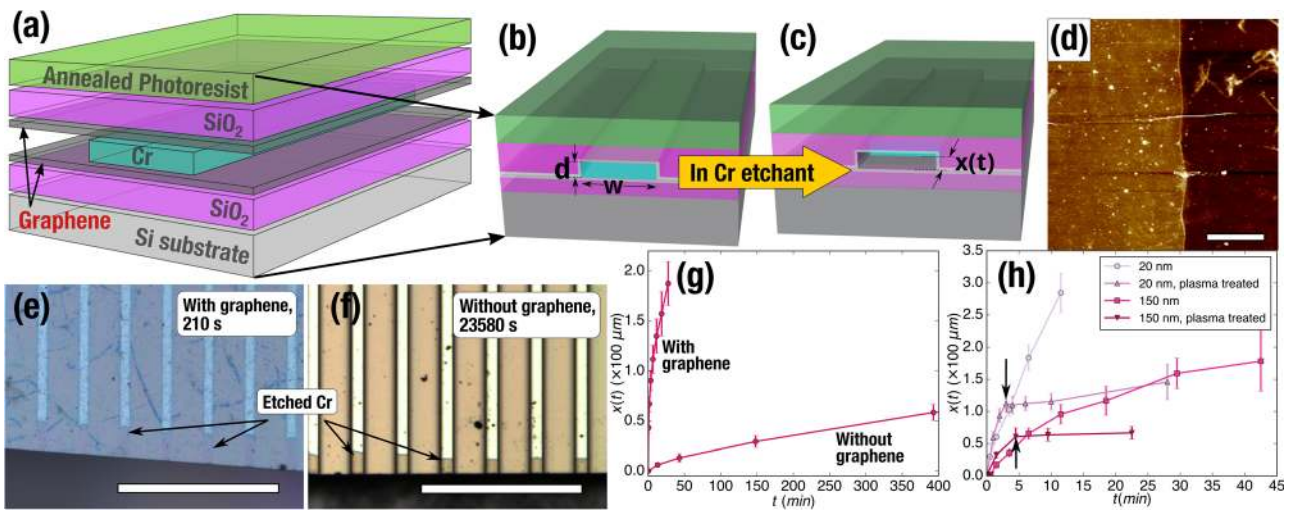

FIG. 1. (a) Different layers used in the samples for Cr etching experiments. (b) Schematic showing graphene lining (thin grey layers) wrapping Cr lines and encapsulated on both sides. The height d and width w of channel are indicated. (c) Cr etchant creates a nanochannel of length $x(t)$ in time t. (d) AFM scan of a sample showing smooth surface of graphene covered Cr line (scale bar is 5 μm). (e) and (f) Optical images of a test ($t = 210$ s, $d = 20$ nm) and a reference ($t = 23\,580$ s, $d = 30$ nm) sample, respectively, with partially etched Cr sacrificial lines (scale bars are 200 μm). Such images were used to extract $x(t)$. (g) The increase in $x(t)$ with time t for the two samples. (h) $x(t)$-t plots showing O_2 plasma exposure slows down the SM removal rate compared to the untreated parts of same samples. The arrows denote time at which plasma was applied.

striking since no chemical reaction takes place. It hints that the transport effects are causing the enhancement.

The removal of SM proceeds by the diffusion of etchant molecules from the mouth of nanochannels to the liquid-solid interface. The etchant molecules dissolve SM, and the products back-diffuse to the bulk etchant from the interface. The higher rate of increase in $x(t)$ in GNCs can be either due to accelerated reaction at the interface or due to faster transport of the reactants and products from the interface. On long time scales, as we are dealing with, the removal rate is expected to be controlled by the diffusion process. This was already indicated in the tapering of the removal rate with time (Figures 1(e) and 1(f)).

The etch profiles generated from a diffusionally controlled process have been analytically treated by Kuiken *et al.*[22] Their analysis, based on Fick's second law, showed that under the assumption that the rate constant for the reaction is large, the etch length $x(t)$ is given by

$$x(t) \sim 0.543B^{-2/3}(Dt)^{1/2}. \quad (1)$$

Here, D is the diffusivity of the etchant molecules and B is a constant that is much greater than unity. According to Equation (1), when the diffusion process governs the form of $x(t)$, the plot of $x(t)$ against $t^{1/2}$ should be a straight line. The slope of the straight line yields the value of diffusivity D, if B is known. For Cr, B is ~1770.[19] For LOR, we use B_{LOR} in the following.

Figure 3(a) plots $x(t)$ vs $\sqrt{t}$ for several thicknesses of Cr lines in GNCs, producing almost straight lines, thus confirming diffusion controlled process. The slopes of lines increase with decreasing thickness, implying that the diffusivities increase with decreasing height of the channels. The reference samples show similar straight lines in $x(t)$ vs $\sqrt{t}$ plots (Figure 3(b)), but the slopes of these straight lines show no trend with change in height of the Cr lines. The diffusivities calculated from these plots are shown in Figure 3(c) as a function of height and width of Cr lines. The enhancement in diffusivities in GNCs is 2–3 orders of magnitudes over the reference channels (Figure 3(c), inset) and is clearly dependent on the height of the channels. The height of the reference channels shows no correlation with the diffusivities in those channels. The width of the channels in either case does not have any effect on the diffusivities. For Cr reference samples, the diffusivities are somewhat higher than the self-diffusivities of water near room temperature ($\sim 3 \times 10^{-5}$ cm^2/s).[23] This match provides a check that the diffusion in nanochannels of reference samples is not significantly different from what one can expect in bulk.

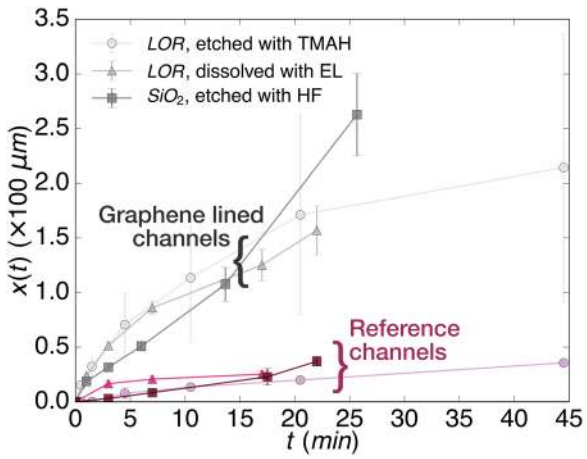

FIG. 2. Comparison of etching of different sacrificial materials in graphene lined (greys) and reference (reds) channels. Chemical reaction with tetramethyl-ammonium hydroxide (TMAH) and physical dissolution in ethyl lactate (EL) after deep UV exposure was used to remove the polymer LOR (lift-off resist). Dilute HF was used to etch SiO_2 lines. In all cases, GNCs offer higher removal rate compared to the reference channels.

Similar observations are valid for sacrificial lines made of LOR etched with TMAH (Figures 3(d)–3(f)). Again, GNCs display higher diffusivities compared to reference samples, and the diffusivities tend to decrease with channel height only for GNCs.

A way to accelerate the diffusion controlled etching process in micro-nanochannels have been demonstrated using galvanic coupled metals.[24,25] In this scheme, the SM line is kept in contact with another metal having lower electrochemical activity and which is exposed to the bulk etchant. During the etching of the nanochannel, the SM is oxidized at the etch front and transported to the channel mouth by diffusion. However, due to the galvanic coupling, the reduction in the etchant can occur on the surface of the low activity metal, far away from the etch front and outside of the channel. Thus, the removal rate only depends on the local concentration, i.e., local solubility, of dissolved SM at the etch front, which can be quite high. The process requires a redox reaction between the SM and etchant and a conductive path to the lower activity metal. The channel dimensions should not affect the removal rates.[25]

The experiments with polymer (LOR) and ceramic (SiO_2) SMs depicted in Figure 2 indicate that galvanic coupling is not the cause of the fast etching in GNCs. Both these materials are electrically insulating, debarring the formation of galvanic pair with graphene. Further, these etch processes do not involve any redox pairs, and the dissolution of LOR with an organic solvent is not even a chemical reaction. The display of fast etching with these materials with same order of magnitude enhancement as Cr implies that changes in physical processes rather than the chemical ones are the reasons for the anomaly.

We suggest that the increase in diffusivities of etchants in GNCs is due to the higher diffusivity of the etchant medium in the vicinity of the graphene surface. A recent theoretical study[12] suggests that clusters of water molecules co-move with the intrinsic ripples in the free-standing graphene. The increase in surface diffusivity comes due to this faster transport of the clusters, yielding 2–3 orders enhancement over self diffusivity in bulk water. The enhancement is similar to the data presented here. It was also suggested that the diffusivity is enhanced as long as there is a coupling between the adsorbates and graphene, implying enhancement for various fluids. Again, our experimental observations of SiO_2 etched in the dilute HF and LOR etched in aqueous TMAH and an organic solvent (EL) is aligned to these predictions. Further experimentation is needed to confirm the realisation of ripple assisted enhancement in fluid diffusivity in GNCs. One can also view the increase in diffusivity as another aspect of the orders of magnitude lower friction[26,27] observed

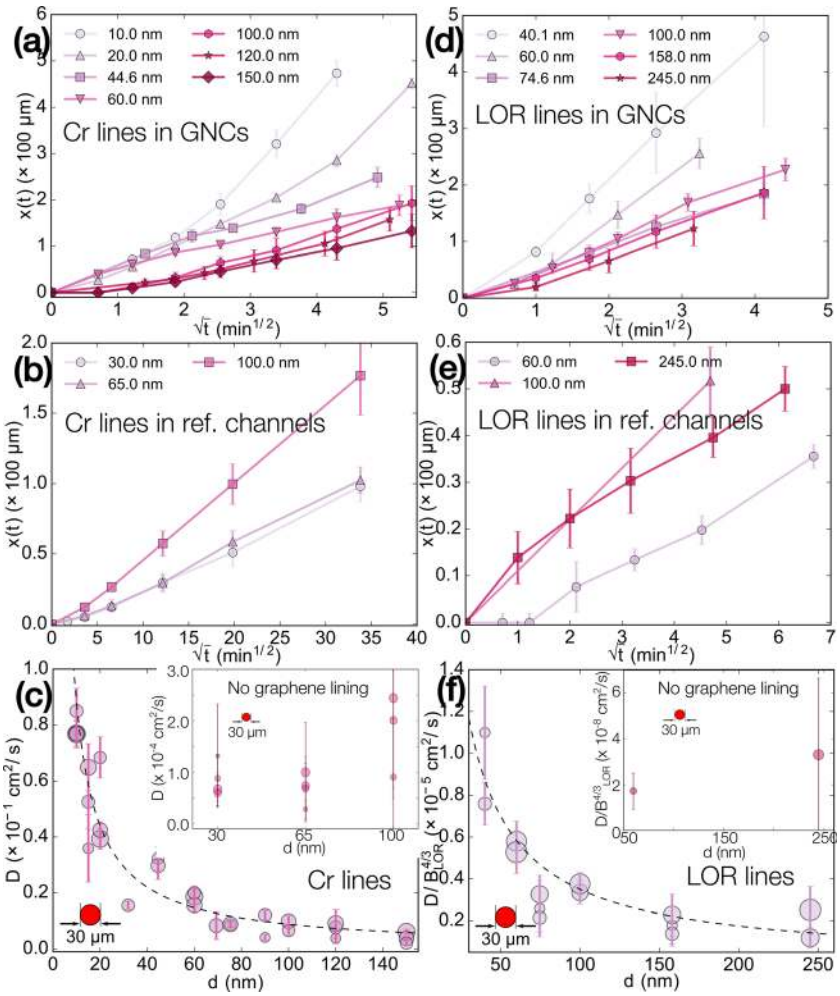

FIG. 3. (a) $x(t)$ plotted against $\sqrt{t}$ for Cr lines in graphene lined nanochannels (GNCs). (b) $x(t)$ plotted against $\sqrt{t}$ for Cr lines in the reference nanochannels. (c) The diffusivities from slopes of $x(t)$ vs $\sqrt{t}$ plots as a function of height d of the nanochannels. The diameter of bubbles indicates the width of Cr lines. The inset shows same data for the reference samples. The dashed curve is trend line plotting $1/d$. (d)–(f) Same data for LOR lines etched with TMAH.

on the graphene surfaces, since diffusivity and dynamic friction are inversely related. This connection can be confirmed by tuning friction, say, by changing strain[28] and observing change in diffusion.

A phenomenological model that encodes the suggestion of high diffusivity of fluids near graphene surface is presented now. Consider the transport of the etchant and the reaction products to and from the liquid-solid interface and the bulk liquid (Figure 4(a)). The diffusive transport is composed of two streams, one in contact with the graphene surface and the other occupying the core of the nanochannel. We assume that the diffusivity of etchant media in the former is D_1 and D_0 in the latter, which is equal to bulk diffusivity of media. We neglect the transport in the direction parallel to the height of the channel.[18] The extent of stream in contact with graphene surface is assumed to be ε ($\leq$d/2), which is independent of the height of the channel. Then, total diffusional flux J, per unit time, across a thin slice of thickness dx, is the sum of liquid diffusing in stream J_1 and that diffusing in the rest of the volume (J_0). Using the standard diffusion equation, we get

$$J = wdD\frac{dc}{dx} = J_1 + J_0$$
$$= (2w\epsilon + 2\epsilon(d-2\epsilon))D_1\frac{dc}{dx} + (w-2\epsilon)(d-2\epsilon)D_0\frac{dc}{dx}. \quad (2)$$

Here, dc/dx is the concentration gradient for the etchant across the slice. The terms in brackets are respective cross-sectional areas of the two streams. Then, the overall diffusivity D is

$$D = \left(\frac{2\epsilon}{d} + 2\frac{\epsilon}{w}\left(1-\frac{2\epsilon}{d}\right)\right)D_1 + \left(1-\frac{2\epsilon}{d}\right)\left(1-\frac{2\epsilon}{w}\right)D_0. \quad (3)$$

As w$\gg$d$>\varepsilon$ in our experiments, we can approximate D

$$D = \left(\frac{2\epsilon}{d}\right)D_1 + \left(1-\frac{2\epsilon}{d}\right)D_0. \quad (4)$$

In other words, D is of the same order of magnitude as D_1 or D_0. The large experimental value of D, which is much large than D_0, implies that $D_1 \gg D_0$, so that the flow is characterized largely by the first term. If so, D is inversely proportional to d, with constant of proportionality of $2\varepsilon D_1$, and the plot of ln(D) vs ln(d) should be a straight line with slope -1. According to these equations, the width of the lines has negligible impact on the removal rates.

The plots in Figures 4(b) and 4(c) demonstrate this to be the case. The logarithm of the observed diffusivities is plotted against thickness of the sacrificial lines in Figures 4(b) and 4(c) for Cr and LOR, respectively. The slopes of these

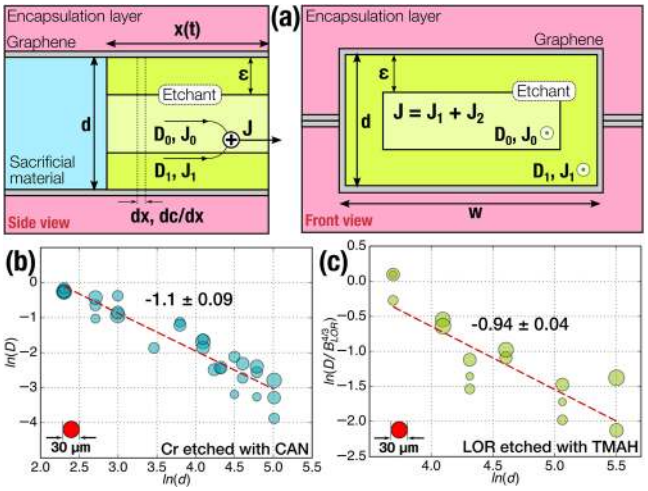

FIG. 4. (a) Side and front views of schematic of the model of transport considered in the text. Two streams J_1 and J_0, characterized by diffusivites D_1 and D_0 are shown, the former confined in a layer of thickness ε near the graphene lining and the latter around the core. Only outgoing diffusive currents are shown. (b) Log-log plot of diffusivity (D) vs. height (d) of the nanochannels for etching of Cr in CAN. The slope of best fit line is shown and the diameter of bubbles corresponds to the width w of the lines. (c) Same plot for LOR etched in TMAH, with the slope of best fit line.

curves are close to -1 and confirm the inverse linear relationship between the two quantities.

We argue in the supplementary material[19] that our observations require ε to be independent of channel height, which in turn implies that only surface effects are responsible for the anomaly. This also implies that when channel height (d) is less than 2ε, the diffusivity should not change with further decrease in channel height. The lowest channel height in our experiments was 15 nm, which restricts ε to $<$7.5 nm, as we do not observe flattening of diffusivity with the decreasing channel height. The constancy of ε is also born out of the ripple driven transport discussed above. In such a scenario, the coupling between the surface movements and the water molecules is effective up to a decay length,[29] given by $(2\xi/\omega)^{1/2}$, where ξ is the kinematic viscosity and ω is the angular frequency of surface oscillations. Using ω of the order of a THz,[29] the decay length comes out to be $\sim$1 nm, which agrees with our observation.

The rationalization of the flow properties using surface effects only is of particular significance. It implies that the anomalous fluid movement near graphitic surfaces is not contingent on confinement. According to our experiments, the increase in confinement (decrease in the nanochannel height) only adds more weight to the surface processes, accentuating their effects.

In conclusion, we have demonstrated a large enhancement in etch rates of SM lines in GNCs. Our data shows that the diffusivities of etchant medium increases by 2–3 orders of magnitude compared to reference channels. A model was proposed for the observed decrease in the enhancement of diffusivities with the increasing channel height. Our experiments can be suitably modified, e.g., by use of electronically controlled doping, modified graphene, or by use of other SM-etchants combinations to investigate this relationship in more detail. Although we have not shown it here, circuits involving GNCs can be made on wafers scale by the standard lithography. This is not easily possible with carbon nanotubes or carbon nanopipes, which despite showing promise for high performance nanofluidic devices have not been used appreciably. We expect GNCs to achieve that promise and germinate new ideas in many areas.

S.K. would like to thank Professor P. Sen and Professor A. K. Singh for helpful discussion. All the authors acknowledge support of DST through TUE project for nanoscience and technology.

[1]J. C. T. Eijkel and A. van den Berg, Microfluid. Nanofluid. **1**, 249 (2005).
[2]H. G. Park and Y. Jung, Chem. Soc. Rev. **43**, 565 (2013).
[3]L. Bocquet and P. Tabeling, Lab Chip **14**, 3143 (2014).
[4]J. K. Holt, H. G. Park, Y. Wang, M. Stadermann, A. B. Artyukhin, C. P. Grigoropoulos, A. Noy, and O. Bakajin, Science **312**, 1034 (2006).
[5]M. Majumder, N. Chopra, R. Andrews, and B. J. Hinds, Nature **438**, 44 (2005).
[6]M. Whitby and N. Quirke, Nat. Nanotechnol. **2**, 87 (2007).
[7]S. Karan, S. Samitsu, X. Peng, K. Kurashima, and I. Ichinose, Science **335**, 444 (2012).
[8]S. C. O'Hern, M. S. H. Boutilier, J.-C. Idrobo, Y. Song, J. Kong, T. Laoui, M. Atieh, and R. Karnik, Nano Lett. **14**, 1234 (2014).
[9]K. Celebi, J. Buchheim, R. M. Wyss, A. Droudian, P. Gasser, I. Shorubalko, J.-I. Kye, C. Lee, and H. G. Park, Science **344**, 289 (2014).
[10]S. P. Surwade, S. N. Smirnov, I. V. Vlassiouk, R. R. Unocic, G. M. Veith, S. Dai, and S. M. Mahurin, Nat. Nanotechnol. **10**, 459 (2015).
[11]M. Majumder, N. Chopra, and B. J. Hinds, ACS Nano **5**, 3867 (2011).
[12]M. Ma, G. Tocci, A. Michaelides, and G. Aeppli, Nat. Mater. **15**, 66 (2016).
[13]R. R. Nair, H. A. Wu, P. N. Jayaram, I. V. Grigorieva, and A. K. Geim, Science **335**, 442 (2012).
[14]H. Huang, Z. Song, N. Wei, L. Shi, Y. Mao, Y. Ying, L. Sun, Z. Xu, and X. Peng, Nat. Commun. **4**, 2979 (2013).
[15]K. I. Bolotin, K. J. Sikes, Z. Jiang, M. Klima, G. Fudenberg, J. Hone, P. Kim, and H. L. Stormer, Solid State Commun. **146**, 351 (2008).
[16]W. Reisner, J. N. Pedersen, and R. H. Austin, Rep. Prog. Phys. **75**, 106601 (2012).
[17]R. Karnik, R. Fan, M. Yue, D. Li, P. Yang, and A. Majumdar, Nano Lett. **5**, 943 (2005).
[18]I. Vlassiouk and Z. S. Siwy, Nano Lett. **7**, 552 (2007).
[19]See supplementary material at http://dx.doi.org/10.1063/1.4943085 for details on growth and transfer of graphene, fabrication and measurement process, impact of removal of samples from the etchant on etch length measurements, calculation of the constant B for Cr etch process and calculation on a variation of model considered in main text.
[20]V. N. Phan, N.-T. Nguyen, C. Yang, P. Joseph, L. Djeghlaf, D. Bourrier, and A.-M. Gue, Langmuir **26**, 13251 (2010).
[21]N. R. Tas, J. Haneveld, H. V. Jansen, M. Elwenspoek, and A. van den Berg, Appl. Phys. Lett. **85**, 3274 (2004).
[22]H. K. Kuiken, J. J. Kelly, and P. H. L. Notten, J. Electrochem. Soc. **133**, 1217 (1986).
[23]R. Mills, J. Phys. Chem. **77**, 685 (1973).
[24]H. Zeng, Z. Wan, and A. D. Feinerman, Nanotechnology **17**, 3183 (2006).
[25]W. Sparreboom, J. C. T. Eijkel, J. Bomer, and A. van den Berg, Lab Chip **8**, 402 (2008).
[26]D. Berman, A. Erdemir, and A. V. Sumant, Carbon **54**, 454 (2013).
[27]T. Filleter, J. L. McChesney, A. Bostwick, E. Rotenberg, K. V. Emtsev, T. Seyller, K. Horn, and R. Bennewitz, Phys. Rev. Lett. **102**, 086102 (2009).
[28]M. Ma, F. Grey, L. Shen, M. Urbakh, S. Wu, J. Z. Liu, Y. Liu, and Q. Zheng, Nat. Nanotechnol. **10**, 692 (2015).
[29]W. Xiong, J. Z. Liu, M. Ma, Z. Xu, J. Sheridan, and Q. Zheng, Phys. Rev. E **84**, 056329 (2011).